How can research on modern and fossil bones help us build more resistant columns?

A Houssaye, Cyril Etienne, Y Gallic, F Rocchia, J Chaves-Jacob

How can research on modern and fossil bones help us build more resistant columns?

Houssaye, A.[1,*], Etienne, C. [1], Gallic, Y. [1], Rocchia, F[2]. & Chaves-Jacob, J.[2]

[1]*UMR 7179 CNRS/Muséum National d'Histoire Naturelle, Département Adaptations du vivant, 57 rue Cuvier CP-55, 75005 Paris, France.*

[2] *Aix Marseille Université, CNRS, ISM, Inst Mouvement Sci, UMR 7287, Marseille, France*

[*]Corresponding author

houssaye@mnhn.fr

Abstract

Bone is an economical material. Indeed, as moving a heavy skeleton is energetically costly, the vertebrate skeleton is adapted to maximise resistance to the stresses imposed with a minimum amount of material, so that bone tissue is deposited where it is needed. Using bone as a source of inspiration should therefore reduce the manufacturing cost (both financial and ecological) and increase the strength (and lifespan) of bioinspired structures. This study proposes to investigate which adaptive features of the outer shape and inner structure of bone, related to compressive strength, could be used to build bioinspired support structures. To do so, we explain the choice of the bones to be analysed and present the results of the biomechanical analyses (FEA) carried out on virtual models built from the structures of the different bone models and of the mechanical tests carried out on 3D-printed versions of these models. The compressive strength of these direct bone bio-inspired columns was compared with each other, and with those of a conventional filled cylindrical column, and of a cylindrical column whose internal structure is bio-inspired from the radius of the white rhinoceros. The results of our comparative analyses highlight that the shape of long bones is less effective than a cylinder in resisting compression but underline the interest in designing bio-inspired cylindrical columns with heterogeneous structures inspired by the radius of the white rhinoceros and the tibia of the Asian elephant, and raise the interest in studying the fossil record using the radius of the giant rhinocerotoid *Paraceratherium*.

Keywords: Bone, skeleton, adaptation, biomechanics, construction, architecture, resistance, paleontology

1. Introduction

Bone is an organic tissue found only in vertebrates. The skeleton forms the framework of the vertebrate body, plays an essential role in protecting organs (e.g. the rib cage for organs such as the lungs and heart, the cranium for the brain), but is also crucial for movement, as it is on the bones that muscles insert, providing rigid lever arms for movement. Bones are thus strongly involved in body support and locomotion. As part of the osteo-muscular system, the skeleton needs to be adapted to the functional constraints faced by the animal during its lifetime. As a consequence, the skeleton bears a strong functional signal in its structure. It achieves this at different scales: 1) in the outer shape of the bones. Indeed, bone morphology strongly varies in shape and proportions pending on functional requirements. The humerus is for example thin and long in a primate, more robust in a horse, and relatively short, flat, and large in a whale [1]; and 2) in their inner structure, that is in the distribution of the osseous tissue inside the bones. The bones of flying birds for example are much lighter than those of terrestrial animals, and secondarily aquatic animals show specific bone structures adapted to cope with a milieu that is not (anymore) dominated by gravity [2]. Although the skeleton is often considered as relatively static, it adjusts along an animal's lifetime pending essentially on its activity. In humans, for example, physical activity is associated with an increase in bone mass whereas bedrest and reduced gravity are associated with bone resorption [3-5]. Bone adaptive changes can naturally be much more intense at an evolutionary scale.

Because of its strong functional signal, bone is thus a powerful and promising tool for bioinspiration, i.e., design approach based on the observation of biological systems used as models [6-7]. The microstructure of bone tissue and its mechanical properties are for instance used to design new materials with hierarchical structures, composites, and even mechano-active materials [8-11]. As for bone architecture, it is particularly well researched in this respect, which notably relies on the fact that bone is an economical material. Indeed, since moving a heavy skeleton is energetically costly, the vertebrate skeleton is adapted to maximise the resistance to the stresses imposed with a minimum amount of material. Bone

is therefore deposited and maintained where it is needed, not where it is not. Using bone as a source of inspiration should therefore optimize stiffness, strength, toughness and lightness, and thus reduce manufacturing cost (both financial and ecological) while increasing the strength (and life span) of bioinspired structures. This explains why bone-inspiration is increasingly used in fields as varied as art, industry, medicine, robotics, garment manufacturing, and architecture (as even in the past in the construction of the Eiffel Tower) [12-18]. This evolution has been facilitated by the recent advances and versatility of additive manufacturing techniques, which allow the creation of objects with increasingly complex microarchitectures [19,20]. The kind of bones used for bioinspiration depend on the mechanical properties of interest. Historically, the focus has been on the human femur [12,21-22]; but since then, inspiration has spread to, for example, the spine for its mix of strength, flexibility and stability [23-25], bird bones for their combination of lightness and strength [13,17,26-27], woodpecker skull and sheep velar bone for impact load applications [28-29], or the relative proportions and articulation of human or other mammalian bones for robotic design [30-31]. However, if bone answers to functional constraints, its structure also relies on developmental and structural (e.g. physical principles), but also historical constraints [32]. Because of the later some structures can have been acquired by selection or genetic drift in the past and have been maintained for various reasons. A structure selected for one function, for example, can later be used for a new one (exaptation) or be maintained even if the function is not ensured anymore (with a low or high degree of vestigiality). In addition, past acquisitions provide different starting points and toolboxes for adapting to one constraint, engendering convergences, i.e. independent responses to a same constraint to ensure a similar function, as exemplified by the wings of pterosaurs (Mesozoic flying reptiles), bats and birds, whose structure is clearly different but which, in all three cases, ensure flight [33]. Moreover, bone structure does not reflect a single functional constraint. Indeed, the skeleton undergoes various constraints during the animal's lifetime; an arm can be involved in various phases and modes of locomotion (e.g., walking, running, climbing, jumping, digging, swimming) but also in grasping, manipulation... As such, the biology bears a mix of adaptive signals and it is required, for a high-quality inspiration, to extract single form-function relationships from this mix, which necessitates to perform comparative analyses in a phylogenetic context. This strengthens the need not only to draw inspiration from nature, but also to collaborate with evolutionary biologists.

In addition, one aspect that should be kept in mind is the relatively small proportion of biodiversity reflected in modern times. Indeed, vertebrates originated about 520 million years ago [34-35] so that there are hundreds of millions of years of evolution of skeletal structures documented in the fossil record. Exploring extinct taxa thus gives access to a much wider spectrum of form-function relationships. Indeed, it naturally strongly extends the range of morphologies, with sometimes very atypical ones (like the paleozoic amphibian *Diplocaulus* with its boomerang-shaped skull, the Mesozoic reptile *Tanystropheus* with its extremely long neck), and more extremes of functions than observed today (like for weight bearing, with the giant sauropod dinosaurs, or for buoyancy control, with extreme increases in bone mass in some Mesozoic marine reptiles, or with extremely high maximum wingspan in some pterosaurs). It also provides access to potential new functions (through e.g., forelimbs adapted to both flight and quadrupedal walking in pterosaurs, the thickened skull of the headbutting pachycephalosaur dinosaurs, or the four-legged aquatic flight of plesiosaurs). Fossil taxa can also enable to reconstruct steps in evolutionary changes, like for the conquest of the terrestrial environment by amphibians, the progressive transition from a terrestrial to an aquatic locomotion in marine mammals and reptiles, or flight acquisition in theropod dinosaurs, which can help to better distinguish the form-function relationships and how they combine. Fossil specimens are sometimes mistakenly thought to be less viable examples because they have become extinct, but most lived for millions of years [36]. Indeed, adaptation is relative and a species can be very well adapted to its environment before a change (climate, predator, competitor) lowers its survivability. Paleobioinspiration is an emerging field. Examples based on the mechanical properties of bones of fossil specimens include the specific bone tissue of the skull dome of the pachycephalosaur dinosaur for impact absorption, the osteoderms of giant glyptodonts (armadillos) for protection through optimized resistance and energy absorption, or the skeleton of pterosaurs (flying reptiles) for flight morphologies [37-39].

Convergences are ideal candidates to study form-function relationships, because they can illustrate different original traits or combinations of adaptive traits that allow a function to be fulfilled, or highlight a single trait/combination in distantly related taxa, as if there could be only one single way to perform the function properly. The combined analysis of these two types of convergence patterns enables to better characterize form-function relationships,

and especially to identify various levels of general biomechanical rules that could be used in bioinspiration.

This work falls within the scope of investigating the structural features of bones of modern and fossil taxa and how they can be used as a source of (paleo)bioinspiration to build more resistant structures. The objective here was to propose new structural designs for columns to increase their strength while minimising their weight. We therefore turned our attention to structural adaptations that would help support significant weight on land, as weight-bearing is the main mechanical function of columns. In modern fauna, only a few terrestrial taxa exhibit particularly high body masses (clearly above a ton): the common hippopotamus, rhinoceroses (except the Sumatran one), and elephants. However, the fossil record encompasses a much higher diversity of forms above one ton, among mammals (e.g., giant herbivores from South America [like *Astrapotherium*], mammoths) and reptiles (various ankylosaurs, stegosaurs and, naturally, sauropods). In order to cautiously characterize form-function relationships, it is necessary to first investigate these relationships in modern forms in order to obtain a solid basis from which to develop them further, thanks to the addition of fossil taxa. The aim here is to present an approach, with its progresses and future developments, that can be used in (paleo)bioinspiration from bones, using the example of the analysis of bone adaptation to support heavy weight. It will thus introduce the considerations and results from biological comparative analyses leading to the choice of the bone models, the results of biomechanical analyses, which are of interest for the following stages and for biology itself, and therefore constitute a win-win interdisciplinary step, as well as the materialisation of these models by 3D printing and the carrying out of mechanical tests, which are directed towards application objectives. It will present how the combination of modelling and mechanical testing enables us to highlight the relative strengths of the different models and to gradually clarify the structural form-function relationships, guiding further research, in order to extract those of interest to propose original bioinspired designs.

2. Choice of the bones of interest

Because limb bones are strongly involved in body support, our analyses focus on limb long bones, from the stylopod (e.g. humerus) and zeugopod (e.g. radius, tibia); the autopod (hand, foot) is more influenced by the nature of the soil on which animals locomote and thus not studied here [40]. Moreover, the relatively more elongated nature of the long bones

appears particularly appropriate to compare their structure and their support efficiency to that of columns.

The choice of the type of bone (e.g., humerus, tibia) to get inspired from is not straightforward. This bone can be a different one pending on the taxon (e.g., species, genus, family) – since adaptive features vary between distinct morphologies – and several bones can be used as models in order to better characterize the form-weight-support relationships from which to draw inspiration. Among massive forms, two main types of limb organization occur. In most taxa, the limbs are flexed when the animal stands. Indeed, even if they can appear rather straight and vertically extended from the outer morphology of the animal, the limb skeleton is not straight. This is not the case for elephants and sauropod dinosaurs whose limbs are said to be columnar, that is that the limb long bones, when standing at rest, are rather vertically oriented. Such taxa are said to be graviportal. This arrangement of the elements is associated with changes of proportion between the different limb elements [41] and a reduction in the moment arm of the ground reaction force on the joints, and therefore a lesser need for muscular strength to keep the joints extended and the animal standing [42] (but combined with reduced locomotor performance and an inability to gallop [43]). The limb bones of graviportal animals could thus appear as the most appropriate ones for comparison with a column. However, if the stylopod bones are flexed in heavy taxa with non-columnar legs, such as the rhinoceroses and hippopotamus, the axes of the zeugopod bones are almost vertical and could also be great comparative models. In ungulates, the forelimbs support about 60% of the animal's weight [44]. Previous studies on the morphological adaptations of the limb long bones of rhinoceroses to weight support have revealed that the radius and ulna are strongly adapted to weight bearing, whereas the tibia is also strongly influenced by the phylogeny [45]. Considering the shape of these bones, the radius of rhinos, being more "cylindrical with larger extremities", appears thus as an interesting comparative model. In elephants, only a few bones display a shape that could be used for comparison with a column. Even if the forelimb is also more involved than the hindlimb in body support [46], the curved shape of the radius is clearly not appropriate for a column, and so is the humerus' shape (being far from showing a cylindrical diaphysis with the deltoid tuberosity and supracondylar crest), although to a lesser extent. In addition, body support is much more split between the radius and the ulna in elephants than in rhinoceroses, so the radius is less dedicated to supporting body weight. As for the ulna, it is

so much involved in triceps traction on the olecranon, that it is not adequate either. Among the hindlimb bones, the tibia has the shape that best fits that of a column [46]. On that basis, three bones were selected for our analyses: 1) the radius of rhinoceroses; 2) the tibia of elephants; 3) the tibia of rhinoceroses, in order to be able to compare results between rhinoceroses and elephants.

3. Material

The five modern species of rhinoceros show clear differences in mass. While all are massive, the extent to which the skeleton is adapted to a heavy support varies markedly between the lightest species, the Sumatran rhino (mean body mass around 775 kg), and the heaviest Indian and white rhinos (mean body mass around 2,000-2,300 kg). Comparing a heavy species with a light species may therefore be worthwhile to better highlight the changes associated with weight support. One radius and one tibia of two male adults from the Sumatran and white rhinoceroses *Dicerorhinus sumatrensis* RBINS 1204 (specimen from the Institut Royal des Sciences Naturelles de Belgique, Brussels, Belgium) and *Ceratotherium simum* NMB 8029 (specimen from the Naturhistorisches Museum Basel, Switzerland) were thus sampled. No such variation occurs in the modern elephants [46]. The tibia of an adult female of *Elephas maximus* MNHN ZM-AC-1983-082 (specimen from the Muséum national d'Histoire naturelle, Paris, France) was sampled. This species is slightly less massive than the African savanna elephant (mean body mass around 2,700 kg in females).

4. Methods

4.1. Scans

Bones were scanned using high-resolution computed tomography at the AST-RX platform of the Muséum National d'Histoire Naturelle, Paris (UMS 2700; GE phoenix|X-ray v|tome|xs 240), with reconstructions performed using DATOX/RES software (phoenix datos|x). Voxel size naturally varies pending on specimen size, from 95 µm in *Dicerorhinus* to 100 µm in *Ceratotherium* and *Elephas*.

4.2. Preparation of the models

Assuming that the main stress applied to a column is compression, the idea here was to ignore the other stresses that naturally apply to the bones when the animal is at rest or moving (e.g., tension of muscular or ligamental origin), and to focus on the resistance of these bones solely to compression. Beyond considering their shape, the approach also involved looking at their inner structure. Bone structure essentially varies according to the thickness and distribution of compact cortical bone, and the distribution, shape, thickness, spacing and orientation of bone trabeculae. Our study deliberately focused on a single parameter in order to explore single form-function relationships. We chose compactness (i.e. fraction of a given volume occupied by bone tissue) because it reflects both the distribution of compact and trabecular bone and is likely to have a major impact on compressive strength (90% of Young's modulus is explained by compactness according to Currey [47]). For that, bone tissue was separated (e.g., from voids and bone marrow) using the Trainable Weka segmentation plugin of imaging processing software ImageJ [48], designed from the Waikato Environment for Knowledge Analysis [49-50]. The segmentation was further refined and checked in VGStudio MAX (v2.2, Volume Graphics Inc.). The segmented bone was further divided into numerous spherical volumes of interest (VOI) within Dragonfly (Object Research Systems, 2021) in order to make 3D cartographies of bone compactness with the BoneAnalysis plugin**.** The spacing of the VOIs (of 1.227 mm for *Dicerorhinus*, 1.219 mm for *Ceratotherium*, and 1.791 mm for *Elephas*) was defined as the sum of the average trabecular thickness and trabecular spacing, and the radius of each VOI as twice the distance of the trabecular spacing (2.454 mm for *Dicerorhinus*, 2.438 mm for *Ceratotherium,* 3.582 mm for *Elephas*). As such, each VOI's diameter should encompass, on average, four trabeculae. Bone volume fraction (BVF) was calculated for each VOI, defining its compactness (between 0 [no bone voxel in the VOI] and 1 [only bone voxels in the VOI]). Three materials were designed based on these cartographies and on the distribution of the VOI compactness (on the histogram): 1) compact cortical bone, with compactness values ranging from 0.85 to 1 (M1); 2) high-density trabecular bone, from 0.5 to 0.85 (M2); and 3) low-density trabecular bone, from 0 to 0.5 (M3). Bones were thus separated into the three materials depending on VOI compactness using the threshold function in Avizo 9.0 (VSG, Burlington, MA, USA), after importing the 3D cartographies as an image stack. Some smoothing was done to reduce the irregularities of the compactness patches and remove the islands, to facilitate the creation of a volumetric mesh for use in Finite Element analyses.

Smoothing had to be carefully balanced in order to reduce the irregularities without affecting the internal geometry (e.g., creating holes in thin part of the materials). The materials, still in image stack form (i.e., voxels) were converted to a surface mesh, which was then corrected (e.g., reducing triangle aspect ratio below 10 and avoiding dihedral angles below 15°), and converted into a single volumetric mesh to import into the FEA software ANSYS.

4.3. Biomechanical analyses

Finite Element Analysis (FEA) enables to study the distribution of stresses and strains inside a complex structure after application of one (or several) constraints (i.e., forces or displacements), by dividing the complex structure into simple tetrahedra. To perform FEA, mechanical properties must be determined for the different materials defined earlier. Young's modulus of elasticity (the stiffness of the material) depends primarily on the material compactness [47]. Young's modulus values were assumed to be similar for the three taxa, previous studies having shown that reasonable simplifications in material property definitions do not impact the gross pattern of deformation [51]. The Young's modulus of the trabecular bone was determined based on a second degree polynomial equation obtained from 14 cubic regions of bone (13 trabecular, 1 cortical) that had been virtually sampled from a segmented bone of *Ceratotherium* and tested for their Young's modulus, using a custom ANSYS routine (see Supplementary Data for details). Using this equation, Young's modulus was attributed to the different materials of the different models (Table 1). Poisson's ratio (describing how much a material deforms perpendicular to the loading direction relative to the axial deformation) was fixed to 0.3 for all osseous materials following Currey [52]. The three materials are in complete contact, with no possibility of movement between them. A vertical constraint was applied at the proximal articular surface (elbow) following the long axis of the bone. Tetrahedra at the distal articulation were blocked in their 6 degrees of freedom (displacements in 3 directions and rotation along 3 axes). To facilitate comparisons between the different models, the same compressive force was applied to all of them, disregarding differences between species and forelimb/hindlimb, initially corresponding to the joint reaction force originating from body weight and transmitted between the carpus and the radius in a white rhinoceros (based on initial OpenSim calculations without muscle inputs from [53]), which was 3467 N. But for the

comparisons to be valuable, the bone models were set to the same volume. For that the volume of osseous tissue (in cm^3) was calculated in order to scale them to the same volume of osseous tissue (and not bone volume) on which the compressive strength was applied. Outer bone cartographies of Von Mises stresses were used to visualize the distribution of the stress intensity on the bones' outer surface, and virtual sections were made to observe stress distribution inside the bones.

In order to compare maximal values of the Von Mises stresses between the various models, we calculated the 95^{th} and 99.9^{th} percentile values, following Walmsley et al. [54].

Table 1. Properties of the bone models with maximal Von Mises stress intensities obtained from FE analyses. E: Young's modulus (MPa)

Bone model	**Bone Volume**	**Osseous tissue's Volume**	**M1**	**M2**	**M3**	**Von Mises Stress**	
	(cm^3)	**(cm^3)**	**(compactness (%), E)**			**(MPa)**	
						95^{th} per.	99.9^{th} per.
Radius *Dicerorhinus*	435	240	95.8 15755	62.3 6362	31.4 1436	6.64	7.40
Radius *Ceratotherium*	1266	785	95.1 15505	62.6 6412	37.3 2098	4.48	4.87
Tibia *Dicerorhinus*	712	360	96.1 15834	60.0 5863	27.5 1068	8.84	9.84
Tibia *Ceratotherium*	1527	876	96.1 15831	65.8 7130	35.0 1819	7.42	8.25
Tibia *Elephas*	3994	2688	95.7 15707	66.3 7257	35.1 1835	7.42	8.04

4.4. Mechanical tests on columns inspired by bones

4.4.a. Direct bone bio-inspired columns

The studied bone geometry, and its compactness distribution, were used to derive bio-inspired columns. These columns were produced using additive manufacturing and then tested in compressive test. Firstly, for comparison efficiency, a scaling of each bone geometry was carried out. This scaling was computed to ensure that all the bones' geometries have the same height (146.6 mm, see figure 1). Naturally, the three-material structure (based on compactness) of each bone (defined previously) was preserved during this scaling step.

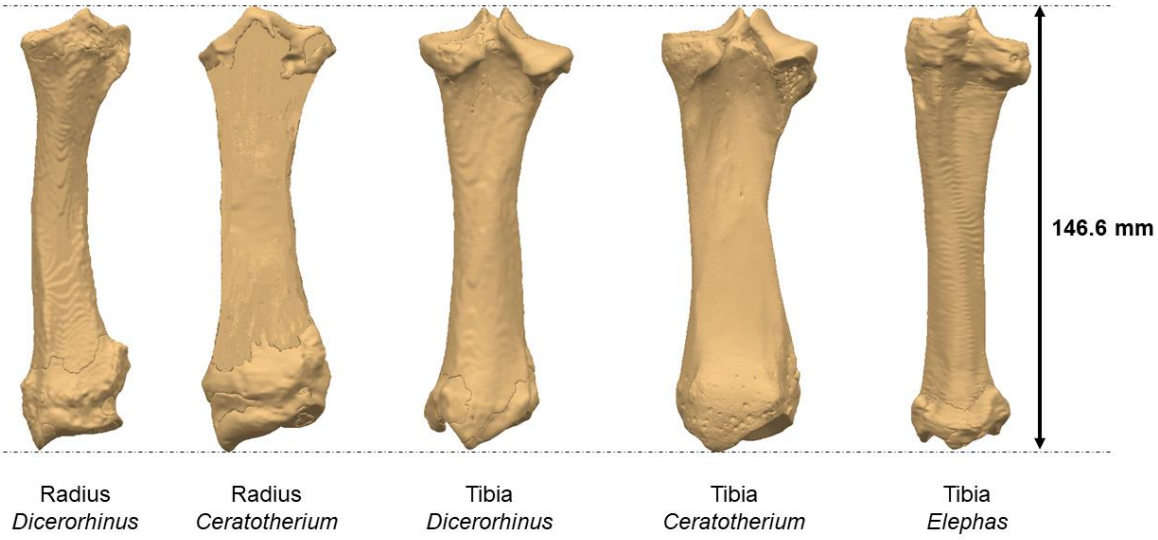

Figure 1. Scaling of the 5 bone's geometry to design bio-inspired columns.

Secondly, specific interfaces were defined to convert bone's geometry into direct bone bio-inspired columns. These interfaces were generated using CATIA V5 Computed Aided Design software. For each scaled bone, the articular surfaces of each epiphysis were isolated and extruded following the long axis of the bone (transition geometry in figure 2). Thereafter, a base plate was added at the extremity of the column to ensure its stability. Total columns' height are 170 mm.

Thirdly, the obtained geometry of each column was prepared for the 3D additive manufacturing using the Ultimaker Cura software. During this preparation, three different geometries were defined in the software with distinct compactness (Table 2):

- Compact material density for compact bone volume (M1), transition geometry, and base plate. Compact material was printed completely filled, without any holes.

- Medium material density for high-density trabecular bone volume (M2). The reduction of density is obtained by leaving porosities in this printed material. The Ultimaker Cura software was used to control the resulting density and thus the proportion of porosities. The pattern used is a 1 mm square grid oriented in the major axis of the column to produce vertical intersecting walls. The thickness of the walls is adapted by the software to provide the specified compactness.
- Low material density for low density trabecular bone volume (M3). The pattern is similar to that of the M2 material, but with a different specified compactness.

Naturally, these three geometries are in contact and will weld during manufacturing. The material density value was defined using the average compactness in each bone volume (see Table 1).

Fourth, the obtained bio-inspired columns were manufactured under the same conditions using plastic filament extrusion on a Volumic STREAM 30 Dual Mk.2. Process parameters are: polylactic acid compound (UNIVERSAL ULTRA - PLC), layer thickness: 0.15 mm, nozzle temperature 235 °C and tray temperature 65 °C. Due to the variation of bones' geometry (and transition geometries accordingly) the volume of each direct bone bio-inspired column varies. Indeed, the bones' geometries were scaled to have the same height, but the other dimensions (length and width) were defined by the natural bone proportion. Furthermore, the repartition and the volume of the 3 materials (M1, M2 and M3) are also defined by the natural bone. Thus, for all these reasons, the mass of each bio-inspired column differs (Table 2).

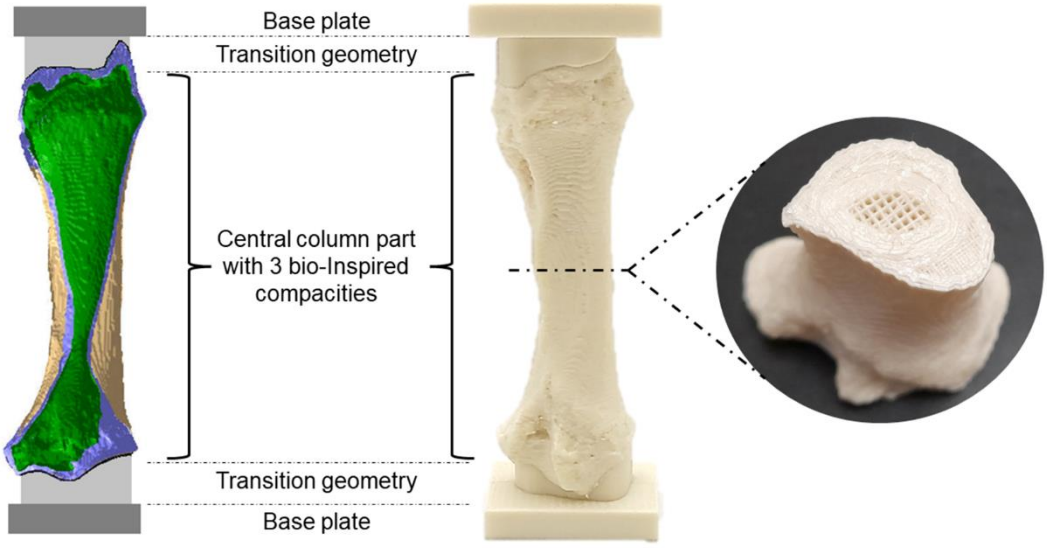

Figure 2. Conception of bone bio-inspired columns.

Table 2. Properties of the columns with maximal effort and stiffness values obtained from the mechanical tests.

Column	**Mass without base plate (g)**	**Material density (%)**			**Max effort (kN)**	**Stiffness (kN/mm)**	**Max effort divided by mass (N/g)**	**Stiffness divided by mass (N/(mm.g))**
		Compact	**Medium**	**Low**				
Radius *Dicerorhinus*	74.5	95.8	62.3	31.4	5.4	3.09	72.6	41.5
Radius *Ceratotherium*	79.5	95.1	62.6	37.3	6.4	2.89	80.4	36.4
Tibia *Dicerorhinus*	94.1	96.1	60.0	27.5	8.7	3.23	92.2	34.4
Tibia *Ceratotherium*	119.4	96.1	65.8	35.0	8.6	3.74	72.2	31.3
Tibia *Elephas*	65.34	95.7	66.3	35.1	7.9	2.34	120.7	35.9
BI column	81.9	95.1	62.6	37.3	19.3	5.82	236.2	71.1
Filled column	157.3	100	NA	NA	38.2	10.52	242.7	66.9

4.4.b. Toward a bioinspired column: “proof of concept” of a bioinspired column

Based on the results of the five direct bone bio-inspired columns and of the filled column, a column with an internal structure bio-inspired from that of the *Ceratotherium* radius (BI column) was designed and tested. This column, presented in figure 3, has a cylindrical external shape and an internal porous geometry. It is composed of three materials like the direct bone bio-inspired columns. The particularity of this internal shape is the “hourglass” bio-inspired shape of the medium and low density areas. Indeed, we assume that in the long bones of heavy species the “hourglass” shape increases the amount of bone material in the diaphysis of the bone where the stress is maximal in a beam submitted to buckling. In the center of the BI column, the thicknesses and densities of the three materials are identical to

those observed in the *Ceratotherium* radius, and the angle of the hourglass is also similar to that observed in the bone.

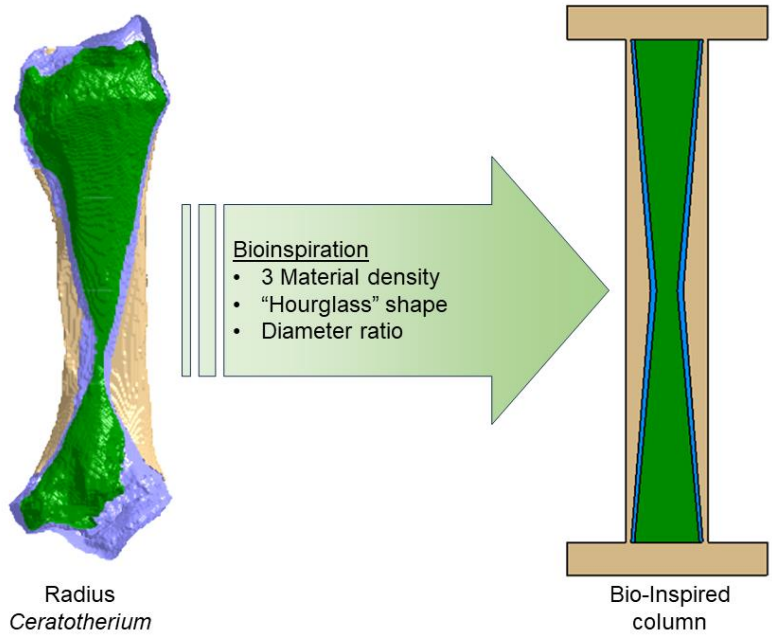

Figure 3. Conception of the column Bio-Inspired from the internal structure of the *Ceratotherium* radius (BI column)

4.4.c. Compressive tests

Compressive tests were carried out on a TEMA PC 400 M 300kN - 4 columns tension - compression test machine. To compare the performance of the different columns, the compressive force/displacement curves obtained were divided by the mass of the column. Thus, the compressive test was carried out on the sevens columns:

- The five direct bone bio-inspired columns;
- The cylindrical bio-inspired (BI) column;
- A filled column. Indeed, to have a reference, and thus compare the strength of the bio-inspired columns with columns as generally constructed, a classical filled cylindrical column, of the same height, was added to the experiments. This column has a full density.

5. Results

5.1. Biomechanical analyses

Radius. A clear difference in the stress distribution occurs between the two rhinoceroses (figures 4; S2-3). In both species, stresses are more intense caudally, which corresponds to the part where the bone is concave. However, these maximal stresses are located medially in *Ceratotherium*, in the distalmost ¾th of the diaphysis, and laterally in *Dicerorhinus*, in the proximal 2/3rd of the diaphysis (figure 4A, D). This is consistent with the radius being concave laterally in *Dicerorhinus*. The maximal intensity on the bone surface is close to 5 MPa in *Ceratotherium* versus 10 MPa for *Dicerorhinus*, whereas the percentiles show more than 2 MPa of difference (Table 1). Mid-sagittal and mid-coronal sections (relatively to the diaphysis) show that stress is relatively poorly intense where compact bone is thickened around the growth center in the diaphysis of *Ceratotherium*, but more intense below this thickening (figure 4C). In *Dicerorhinus*, there is no such thickening and the maximal intensity is closer to the growth center, above the mid-diaphysis (figure 4F). Stress is maximal and more extended in the cortex laterally and then caudally.

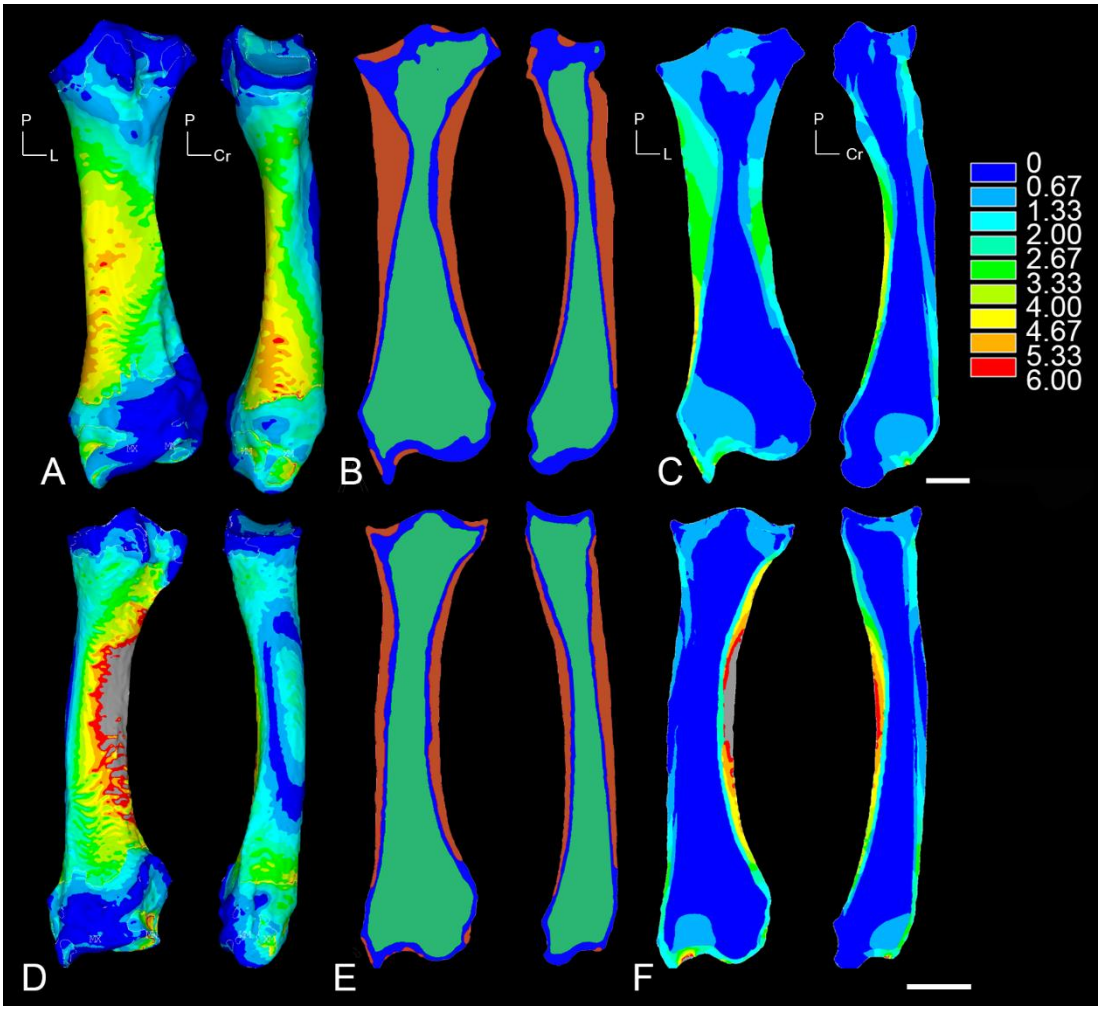

Figure 4. Cartographies of the Von Mises Stress distribution (A, D), coronal (left) and longitudinal (right) sections of the models (B, E) and 2D sections illustrating the Von Mises stress distribution inside the bone (C, F) of the radius of *Ceratotherium* (A, B, C) and *Dicerorhinus* (D, E, F). Color scale in MPa. B, E- Red: M1; Blue: M2; Green; M3. Scale bars equal 4 cm.

Tibia. Stress is more intense in the tibia than in the radius (Table 1; figures 5; S2-3), and more in *Ceratotherium* than in *Dicerorhinus*, with maximal intensities at the surface close to 10 MPa and beyond 12MPa, respectively. Percentiles values show about 2MPa and 3MPa more stress in the radius than in the tibia for *Dicerorhinus* and *Ceratotherium*, respectively, and a lower difference between the taxa (about 1 MPa) than for the radius (Table 1). The highest stress is again in caudal view, in the middle of the distal half of the diaphysis in both taxa, and in the proximo-lateral part of the diaphysis, which are again the concave sides of the bone (figure 5A, D). There is only a slight lateral thickening of the cortex, rather homogeneous along the diaphyseal shaft, in the tibia of *Ceratotherium* (figure 5B, E), so that the stress distribution is rather similar on the longitudinal sections for both taxa (figure 5C, F). Maximal intensity is in the cortex caudo-laterally. Maximal stress in *Elephas* is lower than for *Ceratotherium* for the highest stress values, but equivalent for the 95^{th} percentile (Table 1). Stress distribution appears more homogeneous in caudal view in *Elephas* (figure 5G), but relatively more intense laterally, and medially, in the distal third of the bone, than in *Ceratotherium*, although lateral concavity is not stronger in *Elephas*, whose cranial and lateral borders are straighter than in rhinoceroses (figure S2-3). The surface occupied by Material 2 occupies a larger space in *Elephas* than in the rhinoceroses, except medio-caudally, and notably at the extremities of the epiphyses, which is consistent with *Elephas* tibia supporting more stress in the distal epiphysis than rhinoceroses' (figures 5C, F, I; S2-3).

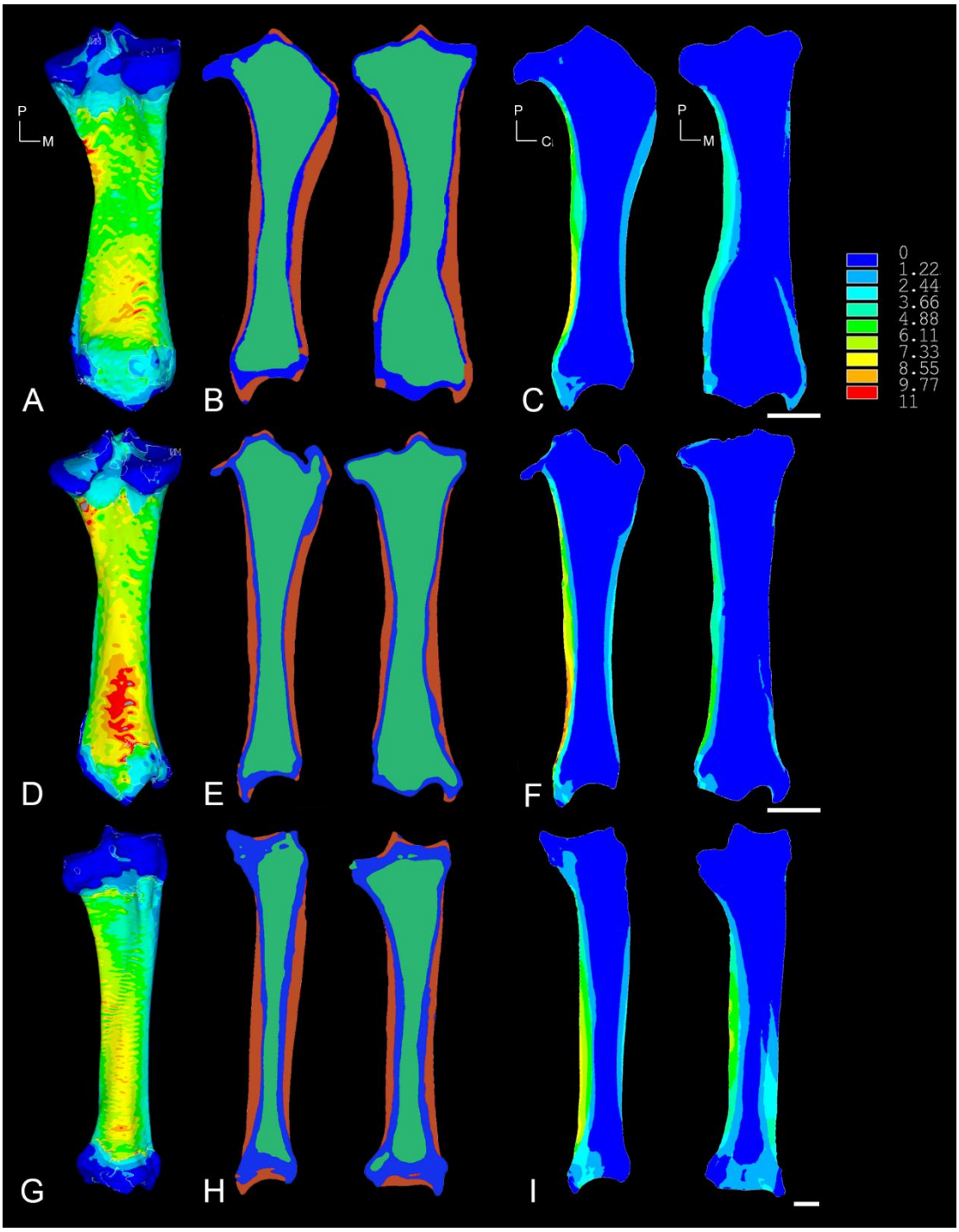

Figure 5. Cartographies of the Von Mises Stress distribution (A, D, G), coronal (left) and longitudinal (right) sections of the models (B, E, H) and 2D sections illustrating the Von Mises stress distribution inside the bone (C, F, I) of the tibia of *Ceratotherium* (A, B, C), *Dicerorhinus* (D, E, F), and *Elephas* (G, H, I). Color scale in MPa. B, E- Red: M1; Blue: M2; Green; M3. Scale bars equal 4 cm.

The histogram clearly shows a smaller area below the curve for *Ceratotherium*'s radius, with much less high stress values than for the other bones (figure 6). Between the other bones, the radius of *Dicerorhinus* appears more resistant than the tibias, the one of *Dicerorhinus* being clearly the least resistant.

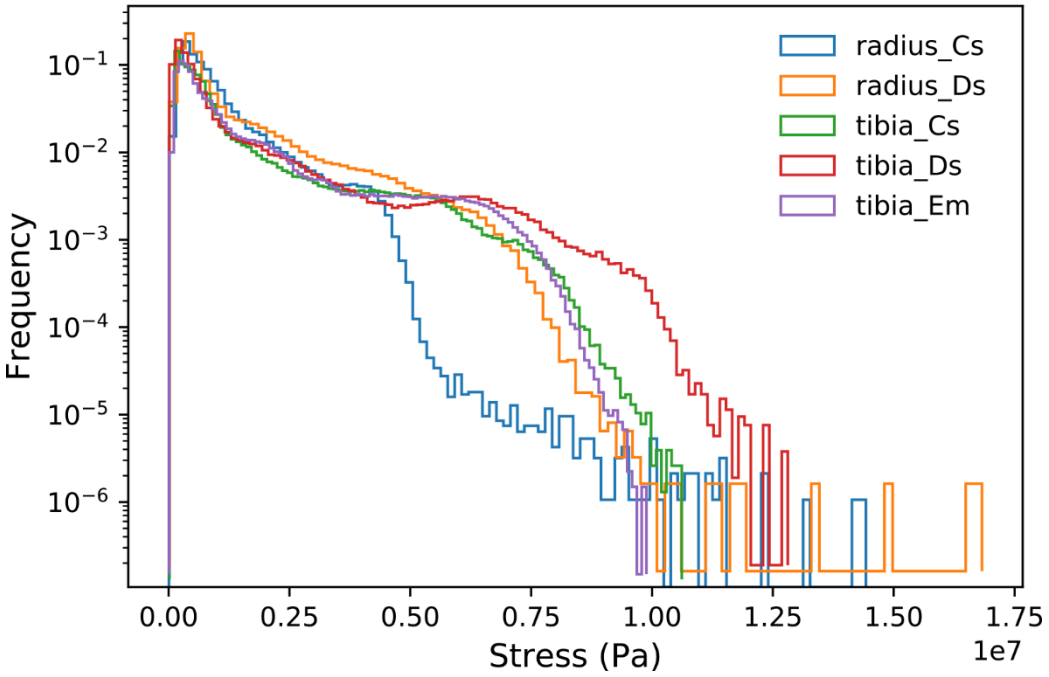

Figure 6. Comparison of the Von Mises stresses for a given volume between the different bone models. Cs: *Ceratotherium simum*; Ds: *Dicerorhinus sumatrensis*; Em: *Elephas maximus*.

5.2. Mechanical tests on columns

The columns inspired from the rhinoceroses's tibias are heavier than the other bio-inspired columns at the same height, whereas the column inspired by the tibia of *Elephas* column is the lightest. The BI column has a weight close to that of the *Ceratotherium* radius column from which it was inspired.

The compressive force/displacement curves divided by the mass of the column (figure 7) highlight a different mechanical behaviour between the radius and tibia direct bone bio-inspired columns. Indeed, the tibia columns endure more displacement (deformation) than the radius ones before failure. This expresses a better resistance to buckling of the tibia columns' geometries. But paradoxically, for the two rhinoceros' species the radius-inspired columns present a better stiffness than tibias-inspired ones. Furthermore, the tibia *Elephas* column presents higher maximal force and displacement before failure than the other ones.

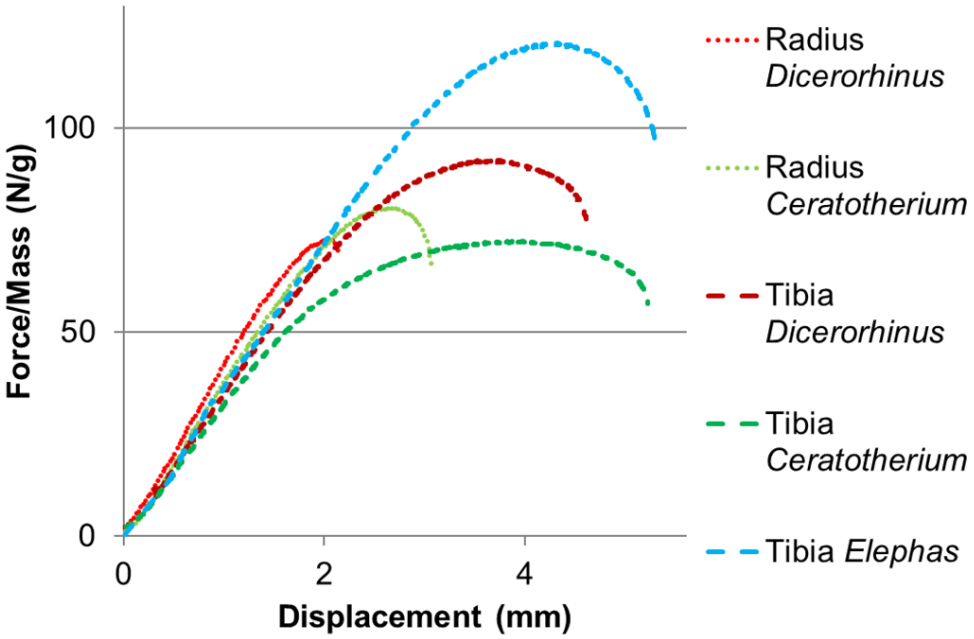

Figure 7. Compressive force/displacement curves divided by the weight of the five tested bio-inspired columns.

The comparison between the filled column and the direct bio-inspired columns clearly shows that the cylindrical filled column is much more efficient in stiffness and maximal force (figure 8). However, the BI column presents a better stiffness than the cylindrical column (gain of 3%), but a maximal effort divided by mass slightly lower (decrease of 6%). Furthermore, the failure mode is completely different: the filled cylindrical column buckles (arches under forces), while the BI column remains straight and breaks under pure compression, with much more deformation before rupture in the bio-inspired column.

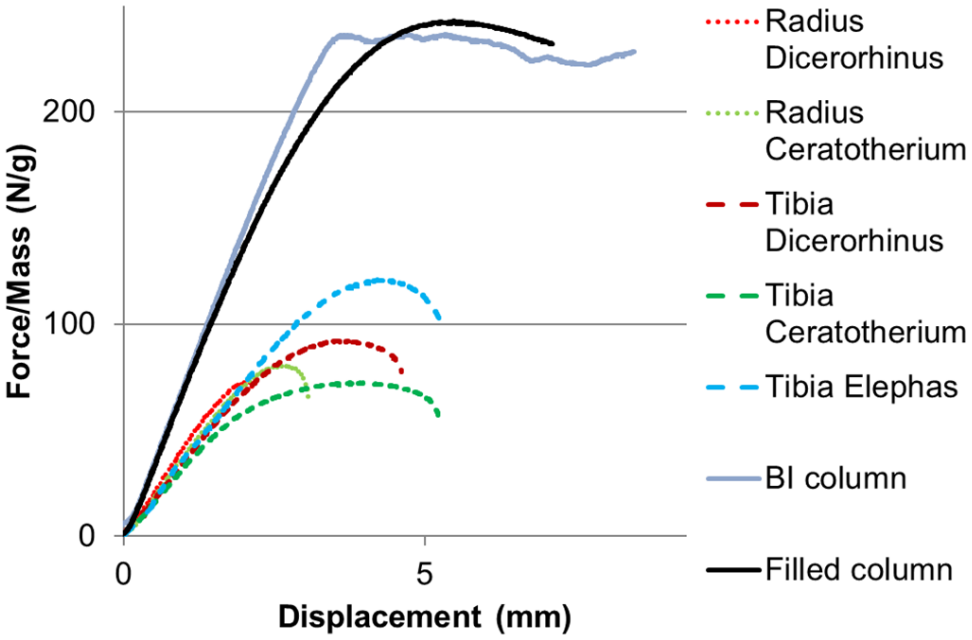

Figure 8. Compressive force/displacement curves divided by the weight of the five tested direct bone bio-inspired columns, BI column, and cylindrical filled column.

6. Discussion

The difference in the stress intensity between the two rhinoceros species shows how the bones of *Ceratotherium* are better adapted to support a heavy weight. The structure of *Ceratotherium* radius diminishes by a factor 1.5 the maximal Von Mises Stresses engendered by the 3500N compressive force as compared to that of *Dicerorhinus*, and the tibia by a factor of about 1.2. This result is in accordance with Mallet et al. [45] who suggested that the radius is strongly adapted for body weight support in rhinoceroses. Maximal stresses are higher in the tibia than in the radius for both taxa, which again confirms that structural adaptations to support a heavy weight in rhinoceroses are stronger in the radius. The structural adaptive features in *Ceratotherium*'s radius, both in shape (e.g. larger epiphyses, straighter diaphysis) and in inner structure (cortical thickening, more compact spongiosa in M3) enable to compensate for a structure that, if proportional to that of *Dicerorhinus*, would have been too weak. *Ceratotherium*'s bones are stockier and the radius is less curved laterally, which probably explains why the maximal constraints are located laterally in *Dicerorhinus* but medially in *Ceratotherium*. But the inner structure does play a role as well. Indeed, if maximal stress intensity in the concave sides of the radius (especially the caudal side) suggests that the bone is submitted to buckling, it is not in the zone of minimal

diaphyseal perimeter that stress is maximal in *Ceratotherium*. This can be explained by this zone being strengthened by a marked increase in bone compactness. The tibia is less concave than the radius, with no marked thickening of the cortex, which could explain why differences are lighter between the two taxa for this bone.

The tibia of *Elephas* shows stress intensities similar to those of *Ceratotherium*'s. The bone is however less stout and more elongated, columnar-shaped, but the inner structure is reinforced by a thicker layer of M2 (M2 and M3 are more compact than in *Dicerorhinus*, but similar between *Ceratotherium* and *Elephas*).

The biomechanical analyses highlight that the maximal stress concentration is on the bone periphery at the level of the diaphysis, close to curvature maxima. This corroborates the mechanical tests which show a buckling failure for all the direct bone bio-inspired columns. Results from the direct bone bio-inspired columns show that they are much less resistant than the classical filled cylindrical column. This result makes sense since a cylindrical structure avoids buckling, which appears as the main cause of fracture of the bio-inspired columns under compression. Indeed, bones' shapes respond to various other constraints than compression, which explains why their specific shape is not optimal for resisting compression. A bioinspired column should thus be cylindrical and not inspired from the external shape of bones. However, such a cylindrical column can be inspired by the internal material distribution and material properties of the direct bone bio-inspired columns. It clearly appears from the mechanical tests that the radius-inspired columns are stiffer than the tibia-inspired ones. Furthermore, the *Elephas* tibia column is clearly much stiffer and more resistant, relatively to its mass, than the two rhinoceroses' tibias-inspired ones. This suggests that the adaptive features of this bone structure (external and internal) are particularly relevant to resist compression. The shape can be involved but microanatomical features, such as the thickness of Material 2, as well. Based on these results, we can regret than elephants do not have radius as strongly involved in body support as rhinoceroses do since such a structure might have been even stiffer in compression than the elephant tibia and thus a better model for bioinspiration. However, this is where the fossil record can be of great interest. Indeed, the giant rhinocerotoid *Paraceratherium* was much heavier than modern elephants, with a mass estimated between 10 and 17 tons [55-56]. This taxon shows relatively long and straight limbs, slender than in modern rhinos although not columnar like in elephants [57]. We might thus expect this taxon to possibly show a radius inner structure

very well adapted to heavy weight support and that could be more efficient than *Ceratotherium*'s.

The first step of bio-inspiration from a heterogeneous inner structure was done here with the column bio-inspired from the inner shape of the *Ceratotherium* radius, the three material distribution (and "hourglass" shape) and properties being bio-inspired. We assumed that this shape was developed in long bones to resist buckling. First experiments conducted in this first version of bio-inspired cylindrical column seem to support this hypothesis. Indeed, in the BI column, the mode of failure was pure compression fracture, while buckling was the mode of failure in all other samples. This first result appears as a positive "proof of concept" of the potential to obtain more resistant columns based on bone bio-inspiration, and further investigations with different internal architectures will further improve the overall outcome.

Therefore, based on our results and notably the probable structural advantage of thickening cortical bone and/or the layer of compact trabecular bone, the next steps would be to: 1) investigate the radius of *Paraceratherium* and 2) build additional cylindrical columns with heterogeneous inner structures differently inspired from *Ceratotherium* radius and *Elephas* tibia, and possibly afterwards from *Paraceratherium* radius. These bio-inspired columns could present the advantage of a lighter inner structure optimized to resist compression with a classical outer shape well adapted to avoid buckling and could thus have the potential to offer more stiffness for a lower amount of material.

Our finite element analyses enabled us to test different architectures. The results on bio-inspired columns are in line with the results of the biomechanical analyses, confirming the value of these upstream analyses in proposing optimal structures, and suggesting that mechanical tests can subsequently be restricted to the strongest models only. Moreover, if our bioinspired columns were printed in plastic, similar differences are naturally to be expected, with varying magnitudes for different polymers, bone-like materials, metals, etc. In addition to compactness, other parameters, such as trabecular bone anisotropy, could be tested subsequently to further improve the quality of the most effective column models obtained.

The form features highlighted to increase compressive strength in this study for static columns could naturally prove useful in moving devices, such as in kinetic architecture or robotics. This is all the more true because, although our study focused on adaptive features

related to heavyweight support/compression, these features in biology could turn out to be useful for other functions too, and could offer improved strength in bending and tension, for example, and not just in compression.

7. Conclusion

This study proposed to investigate how to get inspired from bone structure to build bioinspired supportive columnar structures and to identify the appropriate taxon and bone for this purpose. After having identified possible bioinspiration objects, biomechanical modeling and mechanical tests based on radius and tibias of two rhinoceroses and an elephant have highlighted different morphological and microanatomical structural features associated with body weight support and have raised the interest in investigating the fossil giant rhinocerotoid *Paraceratherium*. This study shows that external bone shape appears much less efficient than a cylinder to support compression, which is consistent with bone shape not being optimized for only compression loads. Furthermore, our experiments highlight a change in the failure mode in the column inspired from *Ceratotherium*'s radius, with buckling suppression. This study thereby proposes a positive proof of concept for cylindrical columns bio-inspired from bone internal structure and suggests that there would be great potential in drawing further inspiration from the internal structure of *Ceratotherium*'s radius, *Elephas*' tibia and the radius of the giant rhinocerotoid *Paraceratherium* to create lighter more resistant bio-inspired columns that will resist buckling.

Acknowledgments

A.H. warmly thanks Thomas Speck for inviting her to the 1st International Conference and Scientific Exhibition on Living Materials Systems and Sonja Seifel for organizing her venue. We are thankful to three anonymous reviewers for their helpful and constructive comments. A.H and J.C-J. acknowledge the CNRS financial support through the MITI Bâtiment et Ville durables and the Défi Biomimétisme.

References

[1] Kardong K 2012 Comparative anatomy, function, evolution. Vertebrates

[2] Canoville A, De Buffrénil V and Laurin M 2021 Bone microanatomy and lifestyle in tetrapods *Vertebrate Skeletal Histology and Paleohistology; De Buffrénil, V., De Ricqlès, AJ, Zylberberg, L., Padian, K., Eds* 724–43

[3] Heinonen A, Oja P, Kannus P, Sievanen H, Haapasalo H, Mänttäri A and Vuori I 1995 Bone mineral density in female athletes representing sports with different loading characteristics of the skeleton *Bone* **17** 197–203

[4] Berg H E, Eiken O, Miklavcic L and Mekjavic I B 2007 Hip, thigh and calf muscle atrophy and bone loss after 5-week bedrest inactivity *European journal of applied physiology* **99** 283–9

[5] Orwoll E S, Adler R A, Amin S, Binkley N, Lewiecki E M, Petak S M, Shapses S A, Sinaki M, Watts N B and Sibonga J D 2013 Skeletal health in long-duration astronauts: nature, assessment, and management recommendations from the NASA bone summit *Journal of bone and mineral research* **28** 1243–55

[6] Felder A, Lewis H, Piker D, Pereira A F and Kestelier X D 2016 Mechano-adaptive space frame generation based on ellipsoid packing Proceedings of IASS Annual Symposia vol 2016 (International Association for Shell and Spatial Structures (IASS)) pp 1–9

[7] Adriaens D 2019 Evomimetics: the biomimetic design thinking 2.0 Bioinspiration, biomimetics, and bioreplication IX vol 10965 (SPIE) pp 41–53

[8] Guo X and Gao H 2006 Bio-Inspired Material Design and Optimization *IUTAM Symposium on Topological Design Optimization of Structures, Machines and Materials* Solid Mechanics and Its Applications ed M P Bendsøe, N Olhoff and O Sigmund (Dordrecht: Springer Netherlands) pp 439–53

[9] Knothe Tate M L, Steck R and Anderson E J 2009 Bone as an inspiration for a novel class of mechanoactive materials *Biomaterials* **30** 133–40

[10] McKittrick J, Chen P-Y, Tombolato L, Novitskaya E, Trim M, Hirata G, Olevsky E, Horstemeyer M and Meyers M 2010 Energy absorbent natural materials and bioinspired design strategies: a review *Materials Science and Engineering: C* **30** 331–42

[11] Giorgio I, Spagnuolo M, Andreaus U, Scerrato D and Bersani A 2020 In-depth gaze at the astonishing mechanical behavior of bone: A review for designing bio-inspired hierarchical metamaterials *Mathematics and Mechanics of Solids* 1–30

[12] Arslan S and Sorguc A 2004 Similarities between structures in nature and man-made structures: biomimesis in architecture *Design and nature* **2** 45–54

[13] Sullivan T N, Wang B, Espinosa H D and Meyers M A 2017 Extreme lightweight structures: avian feathers and bones *Materials Today* **20** 377–91

[14] Du Plessis A, Broeckhoven C, Yadroitsava I, Yadroitsev I, Hands C H, Kunju R and Bhate D 2019 Beautiful and functional: a review of biomimetic design in additive manufacturing *Additive Manufacturing* **27** 408–27

[15] Ghazlan A, Nguyen T, Ngo T and Linforth S 2020 Performance of a 3D printed cellular structure inspired by bone *Thin-Walled Structures* **151** 106713

[16] He J and Gao F 2020 Mechanism, actuation, perception, and control of highly dynamic multilegged robots: A review *Chinese Journal of Mechanical Engineering* **33** 1–30

[17] Buccino F, Aiazzi I, Casto A, Liu B, Sbarra M C, Ziarelli G, Vergani L M and Bagherifard S 2021 Down to the bone: A novel bio-inspired design concept *Materials* **14** 4226

[18] Buccino F, Bruzzaniti P, Candidori S, Graziosi S and Vergani L M 2022 Tailored Torsion and Bending-Resistant Avian-Inspired Structures *Advanced Engineering Materials* **24** 2200568

[19] Gibson I, Rosen D, Stucker B and Khorasani M 2021 Development of Additive Manufacturing Technology *Additive Manufacturing Technologies* ed I Gibson, D Rosen, B Stucker and M Khorasani (Cham: Springer International Publishing) pp 23–51

[20] du Plessis A, Babafemi A J, Paul S C, Panda B, Tran J P and Broeckhoven C 2021 Biomimicry for 3D concrete printing: A review and perspective *Additive Manufacturing* **38** 101823

[21] Audibert C, Chaves-Jacob J, Linares J-M and Lopez Q-A 2018 Bio-inspired method based on bone architecture to optimize the structure of mechanical workspieces *Materials & Design* **160** 708–17

[22] Shen Y and Liu Y 2022 Bioinspired building structural conceptual design by graphic static and layout optimization: a case study of human femur structure *Journal of Asian Architecture and Building Engineering* **21** 1762–78

[23] Galbusera F and Bassani T 2019 The spine: a strong, stable, and flexible structure with biomimetics potential *Biomimetics* **4** 60

24] Golkar N, Sadeghpour A and Divandari J 2021 Drawing inspiration from the spine, designing a pedestrian bridge [spine-inspired design of a pedestrian bridge] *Journal of Architecture and Urbanism* **45** 119–30

[25] Sun X, Wang F and Xu J 2021 A novel dynamic stabilization and vibration isolation structure inspired by the role of avian neck *International Journal of Mechanical Sciences* **193** 106166

[26] Ripley R L and Bhushan B 2016 Bioarchitecture: bioinspired art and architecture—a perspective *Philosophical Transactions of the Royal Society A: Mathematical, Physical and Engineering Sciences* **374** 20160192

[27] Zhang S, Li J, Bi C, Wang Z, Tang D and Tang H 2023 Design and load-bearing capacity analysis of bone-inspired lightweight microstructures

[28] Jung J, Pissarenko A, Trikanad A A, Restrepo D, Su F Y, Marquez A, Gonzalez D, Naleway S E, Zavattieri P and McKittrick J 2019 A natural stress deflector on the head? Mechanical and functional evaluation of the woodpecker skull bones *Advanced Theory and Simulations* **2** 1800152

[29] Aguirre T G, Fuller L, Ingrole A, Seek T W, Wheatley B B, Steineman B D, Donahue T L H and Donahue S W 2020 Bioinspired material architectures from bighorn sheep horncore velar bone for impact loading applications *Scientific Reports* **10** 18916

[30] Ananthanarayanan A, Azadi M and Kim S 2012 Towards a bio-inspired leg design for high-speed running *Bioinspir. Biomim.* **7** 046005

[31] Liu C, Moncada A, Matusik H, Erus D I and Rus D 2023 A Modular Bio-inspired Robotic Hand with High Sensitivity *2023 IEEE International Conference on Soft Robotics (RoboSoft)* pp 1–7

[32] Gould S J 2002 *The structure of evolutionary theory* (Harvard University Press)

[33] Romanes G J 1892 *Darwin and After Darwin: The Darwinian theory. 1892* vol 1 (Open court publishing Company)

[34] Shu D G, Luo H, Conway Morris S, Zhang X, Hu S, Chen L, Han J, Zhu M, Li Y and Chen L 1999 Lower Cambrian vertebrates from south China *Nature* **402** 42–6

[35] Yang C, Li X-H, Zhu M, Condon D J and Chen J 2018 Geochronological constraint on the Cambrian Chengjiang biota, South China *Journal of the Geological Society* **175** 659–66

[36] Howe S P and Shyam V 2022 Inspiration from paleomimetics: Fossil does not equal failure *Biomimicry for Materials, Design and Habitats* (Elsevier) pp 123–38

[37] Chatterjee S, Roberts B and Lind R 2010 Pterodrone, a pterodactyl-inspired unmanned air vehicle that flies, walks, climbs, and sails *WIT Transactions on Ecology and the Environment* **138** 301–16

[38] Du Plessis A, Broeckhoven C, Yadroitsev I, Yadroitsava I and le Roux S G 2018 Analyzing nature's protective design: the glyptodont body armor *Journal of the Mechanical Behavior of Biomedical Materials* **82** 218–23

[39] Martin-Silverstone E, Habib M B and Hone D W 2020 Volant fossil vertebrates: potential for bioinspired flight technology *Trends in Ecology & Evolution* **35** 618–29

[40] Hanot P, Herrel A, Guintard C and Cornette R 2017 Morphological integration in the appendicular skeleton of two domestic taxa: the horse and donkey *Proceedings of the Royal Society B: Biological Sciences* **284** 20171241

[41] Osborn H F 1929 *The titanotheres of ancient Wyoming, Dakota, and Nebraska* vol 55 (US Government Printing Office)

[42] Biewener A and Patek S 2018 *Animal locomotion* (Oxford University Press)

[43] Ren L, Miller C E, Lair R and Hutchinson J R 2010 Integration of biomechanical compliance, leverage, and power in elephant limbs *Proceedings of the National Academy of Sciences* **107** 7078–82

[44] Hildebrand M, Goslow G E and Hildebrand V 2001 *Analysis of vertebrate structure* vol 2 (Wiley New York)

[45] Mallet C, Cornette R, Billet G and Houssaye A 2019 Interspecific variation in the limb long bones among modern rhinoceroses—extent and drivers *PeerJ* **7** e7647

[46] Bader C, Delapré A and Houssaye A 2023 Shape variation in the limb long bones of modern elephants reveals adaptations to body mass and habitat *Journal of Anatomy* **242** 806–30

[47] Currey J D 2006 *Bones: structure and mechanics* (Princeton university press)

[48] Schindelin J, Arganda-Carreras I, Frise E, Kaynig V, Longair M, Pietzsch T, Preibisch S, Rueden C, Saalfeld S and Schmid B 2012 Fiji: an open-source platform for biological-image analysis *Nature methods* **9** 676–82

[49] Hall M, Frank E, Holmes G, Pfahringer B, Reutemann P and Witten I H 2009 The weka data mining software: An update, software available at http://www. cs. waikato. ac. nz/ml/weka *SIGKDD explorations* **11**

[50] Arganda-Carreras I, Kaynig V, Rueden C, Eliceiri K W, Schindelin J, Cardona A and Sebastian Seung H 2017 Trainable Weka Segmentation: a machine learning tool for microscopy pixel classification *Bioinformatics* **33** 2424–6

[51] Richmond B G, Wright B W, Grosse I, Dechow P C, Ross C F, Spencer M A and Strait D S 2005 Finite element analysis in functional morphology *The Anatomical Record Part A: Discoveries in Molecular, Cellular, and Evolutionary Biology: An Official Publication of the American Association of Anatomists* **283** 259–74

[52] Currey J D 2002 Bones: structure and mechanics *Princeton New Jersey Press, Princeton, NJ*

[53] Etienne C, Houssaye A, Fagan M and Hutchinson J R In review Estimation of the forces exerted on the limb long bones of a White Rhinoceros (*Ceratotherium simum*) using musculoskeletal modelling and simulation *Journal of Anatomy*

[54] Walmsley C W, McCurry M R, Clausen P D and McHenry C R 2013 Beware the black box: investigating the sensitivity of FEA simulations to modelling factors in comparative biomechanics *PeerJ* **1** e204

[55] Fortelius M and Kappelman J 1993 The largest land mammal ever imagined *Zoological Journal of the Linnean Society* **108** 85–101

[56] Larramendi A 2015 Shoulder height, body mass, and shape of proboscideans *Acta Palaeontologica Polonica* **61** 537–74

[57] Mallet C, Billet G, Cornette R and Alexandra Houssaye A 2022 Adaptation to graviportality in Rhinocerotoidea? An investigation through the long bone shape variation in their hindlimb *Zoological Journal of the Linnean Society* zlac007

Data availability statement

The scans of the five bones analysed in this study are available upon request from MNHN's 3Dthèque (https://3dtheque.mnhn.fr/).